https://doi.org/10.5194/egusphere-2026-308
Preprint. Discussion started: 13 February 2026

Dust Transport and Local Anthropogenic Emissions Differently Shape Atmospheric Ice-Nucleating Particles: Insights from an Industrial Urban Atmosphere

Jiawei Yang[1], Jingchuan Chen[1], Jie Chen[2], Zeyu Feng[1], Wenxu Fang[1], Yanting Qiu[1], Junrui Wang[1], Ruiqi Man[1], Taomou Zong[1], Zhijun Wu[1,3,*], Ning Tang[4], Min Hu[1]

[1]State Key Laboratory of Regional Environment and Sustainability, International Joint Research Center for Atmospheric Research (IJRC), Institute of Carbon Neutrality, College of Environmental Sciences and Engineering, Peking University, 100871, Beijing, China
[2]Institute for Atmospheric and Climate Science, ETH Zürich, Zurich, 8092, Switzerland
[3]Collaborative Innovation Center of Atmospheric Environment and Equipment Technology, Nanjing University of Information Science and Technology, Nanjing 210044, China
[4]Institute of Nature and Environmental Technology, Kanazawa University, Kanazawa, Japan

Correspondence to: Zhijun Wu (zhijunwu@pku.edu.cn)

Abstract. Atmospheric ice-nucleating particles (INPs) are vital for cloud formation, yet the importance of INPs from anthropogenic sources remains poorly understood. We conducted a month-long winter field campaign in Taiyuan, a heavily industrialized city, to quantify INP concentrations (N_{INP}) and ice nucleation active site density (n_s) of immersion mode INPs, alongside particle size distributions and chemical compositions. Our results indicate that N_{INP} ranged from 0.0532 to 13.4 L^{-1} at −15 °C, corresponding to n_s values of 10^5–10^7 m^{-2}. During a dust event, both N_{INP} (7.47 L^{-1} ; 95% CI: 6.64–8.41 L^{-1}) and n_s (1.77×10^7 m^{-2} ; 95% CI: 1.58–1.99 × 10^7 m^{-2}) increased nearly one order of magnitude compared with periods without natural dust influence (1.75 L^{-1} and 3.89×10^6 m^{-2}, respectively), highlighting the dominance of long-range transported desert dust. In contrast, during pollution periods, N_{INP} showed only weak correlations with urban aerosol components like SO_4^{2-}, NO_3^-, and OC ($|r| < 0.3$). Positive matrix factorization (PMF) identified five $PM_{2.5}$ sources: coal combustion and traffic emissions, industry, (anthropogenic) dust, secondary aerosols and fireworks. Although these dominated the $PM_{2.5}$ mass, none contributed significantly to INPs. This implies that even in heavily industrialized environments, the direct impact of anthropogenic emissions on INP loading remains limited. In summary, long-range mineral dust transport is the decisive driver of INP enhancements, while traditional anthropogenic fine aerosols contribute minimally. Observed N_{INP} variability is likely governed by the interplay of episodic coarse-mode inputs and atmospheric processing rather than a single dominant source.

Short summary

Clouds contain supercooled water that needs microscopic "seeds" called ice-nucleating particles (INPs) to freeze into ice. We investigated if pollution in Taiyuan, an industrial city, acts as these INPs. Surprisingly, despite heavy smog or haze, local emissions contributed little to ice formation. Instead, natural dust from distant deserts was the main driver. This implies that even in heavily polluted environments, natural dust rather than human activity governs cloud freezing processes.

https://doi.org/10.5194/egusphere-2026-308
Preprint. Discussion started: 13 February 2026

1 Introduction

Atmospheric ice-nucleating particles (INPs) play a critical role in cloud formation, cloud radiative properties and precipitation through heterogeneous ice nucleation (Lohmann and Feichter, 2005; IPCC, 2014; Lohmann et al., 2016). Although INPs constitute a minute fraction of ambient aerosols under natural conditions (approximately 1 in 10^5 ambient particles in the free troposphere (DeMott et al., 2010)), their ability to modulate cloud properties and lifetimes has received substantial scientific interest. Heterogeneous ice nucleation is generally understood to occur through four mechanisms: deposition ice nucleation, condensation freezing, immersion freezing and contact freezing (Hoose and Möhler, 2012; Vali et al., 2015). Among these, immersion freezing has been widely reported to be the most important ice nucleation mechanism for mixed-phase clouds (Ansmann et al., 2008; Murray et al., 2012; Westbrook and Illingworth, 2013).

The urban atmosphere is characterized by intensive anthropogenic activities, diverse aerosol emission sources, elevated aerosol loadings, and complex chemical compositions. However, the key factors controlling atmospheric INP concentrations in such environments, including aerosol composition, size, and source characteristics, remain uncertain (Kanji et al., 2017). Previous studies in Beijing and Tokyo demonstrated that INP concentrations often show no significant correlations with black carbon (BC) or $PM_{2.5}$ mass, or the number concentration of particles larger than 0.5 μm during air pollution episodes (Chen et al., 2018; Tobo et al., 2020; Zhang et al., 2022). This suggests that typical urban pollution aerosols are generally inefficient INPs.

However, this observation contrasts with laboratory findings, which have identified several anthropogenic aerosol types as potential INPs. Soot and fly ash from incomplete combustion can exhibit significant activity under immersion freezing; for instance, fly ash from coal-fired power plants has been observed to initiate freezing near −22 °C. Industrial processes also release ice-active particles, including metallic compounds (e.g., Fe, Cu, Ni) from metal smelting and manufacturing, as well as mineral dust from cement, asphalt, and fertilizer production (Toll et al., 2024). Moreover, biomass burning represents another potential source, with agricultural fires near Mexico City reported to induce freezing at temperatures above −15 °C, likely due to the presence of associated biological particles (McCluskey et al., 2014; Jahn et al., 2020; Cabrera-Segoviano et al., 2022). The complexity of urban INPs is further exemplified by observations in New Delhi, where INP concentrations correlated moderately ($r = 0.52$) with BC during fog episodes, indicating that particle composition and meteorological conditions may modulate INP activity (Wagh et al., 2021). This gap between laboratory potential and field observations indicates that urban INP variability may be governed by specific high-efficiency contributors rather than total aerosol mass or number concentrations. Therefore, mineral dust and biological particles, which have long been established as the most potent atmospheric INPs, require careful consideration even in heavily industrialized areas.

Mineral dust is widely recognized as the most important atmospheric INP due to its vast global emissions, estimated at up to ~5000 Tg yr^{-1} (Engelstaedter et al., 2006). Its intrinsically high ice-nucleating activity at temperatures below −8 °C is primarily attributed to specific mineral components such as K-feldspar, which has been systematically identified as a key active species in laboratory settings (Atkinson et al., 2013; Augustin-Bauditz et al., 2014; Zolles et al., 2015). In the context

https://doi.org/10.5194/egusphere-2026-308
Preprint. Discussion started: 13 February 2026

of East Asia, mineral dust transported from northwestern deserts serves as a decisive driver of INP enhancements in downwind urban areas, exhibiting efficiencies comparable to those of Saharan dust (Price et al., 2018; Reicher et al., 2019; Chen et al., 2021). Furthermore, the influence of dust in cities is not limited to long-range natural transport; anthropogenic dust—such as agricultural operations, construction, and other urban processes—can also contribute substantially to atmospheric INPs in urban and peri-urban regions (Chen et al., 2024).

In comparison to mineral dust, aerosols of biological origin, such as pollen, fungal spores, proteins, and other macromolecular organics can nucleate ice at relatively warmer temperatures, often above −15 °C (Pummer et al., 2015; Polen et al., 2016; Kanji et al., 2017). While these bioaerosols may be less abundant by mass than mineral dust, their exceptional ice-nucleating efficiency means that even a small population can dominate the urban INP budget at the early stages of cloud glaciation.

Although considerable progress has been made in identifying both natural and anthropogenic sources of atmospheric INPs, their formation pathways and source attributions in urban environments remain poorly constrained due to the complex mixture of aerosol types and variable emission patterns. To address this gap, a comprehensive winter field campaign was conducted in Taiyuan, a representative industrial city in northern China, over a one-month period. Taiyuan frequently experiences severe particulate pollution and episodic dust events, positioning it as an ideal location to investigate the combined effects of anthropogenic and natural emissions. In this study, number concentration of immersion mode INP (N_{INP}) and the number of active sites per unit surface area of INPs (n_s) were measured under mixed-phase cloud conditions (from −35 °C to −5 °C) concurrently with size distribution and chemical composition of aerosol particles, and meteorological parameters. Source apportionment of $PM_{2.5}$ using a positive matrix factorization (PMF) model enabled the identification of major emission sources and their temporal variations.

2 Methods

2.1 Sampling

Taiyuan is a major industrial city in northern China, often experiencing elevated concentrations and enrichment factors (EFs) of $PM_{2.5}$-bound heavy metals, influenced by local emissions, regional transport, and complex terrain (Li et al., 2021). A winter observation campaign was conducted from 3 December 2023 to 14 January 2024, coinciding with the centralized heating season characterized by intensive coal combustion. The sampling site (37.88° N, 112.55° E) is located on the rooftop (~20 m above ground level) of a four-story building at the Taiyuan Municipal Ecology and Environment Bureau. Situated near Taoyuan 3rd Alley, this site is representative of a typical central urban environment. Although it is removed from direct major industrial point sources, it remains suitable for monitoring urban fine particulate pollution driven by mixed anthropogenic activities.

Key atmospheric pollutants were continuously monitored at the station, including concentrations of water-soluble ions, heavy metals, elemental carbon (EC) and organic carbon (OC), gas concentrations (SO_2, NOx, O_3, CO), particulate matter

https://doi.org/10.5194/egusphere-2026-308
Preprint. Discussion started: 13 February 2026

concentrations ($PM_{2.5}$ and PM_{10}), together with meteorological parameters (wind speed, wind direction, temperature, relative humidity, and atmospheric pressure). In addition, a two-channel sampler was used to collect particles on filters for INP measurement. INP filter samples were collected on polycarbonate filters (47 mm, Nuclepore Track-Etch Membrane, 0.2 µm pore size, Whatman) using a two-channel sampler without a cyclone, from 4 December 2023 to 5 January 2024. The sampling flow rate was maintained at 6 L min^{-1} by a mass flow controller (MFC), with a 24 h sampling duration. Considering flow fluctuations and filter switching time, the total sampled air volume for each filter was approximately 8000 L. Except for the filter samples, all observation data were recorded as hourly averages.

2.2 Instrumentation

2.2.1 Particle mass and size distribution measurement

Mass concentrations of particulate matter (PM) with aerodynamic diameter (d_a) smaller than 2.5 and 10 µm ($PM_{2.5}$ and PM_{10}, respectively) were measured by a tapered element oscillating microbalance (TEOM) monitor.

Two scanning mobility particle sizer (SMPS) systems were employed to measure particle number size distributions in the 2.02–514 nm range during the campaign, while the range of data used in this study was 3–453 nm. The first system consisted of a TSI Classifier 3080 with Differential Mobility Analyzer (DMA) 3085 and Condensation Particle Counter (CPC) 3776, while the second system included a TSI Classifier 3082 with DMA 3081 and CPC 3772. Sample humidity was regulated using a Nafion^{TM} membrane dryer (Perma Pure, MD-700-24F-3) to prevent water vapor condensation. Multiple charging corrections were applied during data processing (Wiedensohler, 1988).

An Optical Particle Counter (Aerosol Spectrometer and Dust Monitor 1.108, Grimm Aerosol Technik) was used to obtain number size distribution (PNSD) of particles ranging from 0.5 to 20 µm in optical-equivalent diameters. Estimating d_a from optical-equivalent diameter typically requires knowledge of particle complex refractive index and morphological parameters (e.g., dynamic shape factor). In this study, neither refractive index nor morphology were measured independently. Accordingly, using optical diameter as a surrogate for d_a introduces unavoidable uncertainties and potential biases (Peters et al., 2006). Moreover, when converting d_a to mobility diameter (d_m), we assumed an effective particle density of 1.5 g cm^{-3} and a shape factor of unity. This assumption may also lead to uncertainty in the reported d_m, particularly in the coarse-mode size range (Huang et al., 2021).

2.2.2 Particle chemical composition

The water-soluble inorganic ions in $PM_{2.5}$ were measured in-situ using a Monitor for AeRosols and Gases in ambient Air (MARGA 1S; Metrohm AG, Switzerland). The analysis focused on major inorganic ions, including NO_3^-, SO_4^{2-}, NH_4^+, Cl^-, K^+, Ca^{2+}, Na^+ and Mg^{2+}. In parallel, the MARGA simultaneously measured the gaseous pollutants including SO_2, HNO_2, HNO_3, NH_3, and HCl. EC and OC concentrations were determined using a Carbonaceous Aerosol Speciation System (CASS; Aerosol d.o.o., Slovenia, EU) (Rumsey et al., 2014; Rumsey and Walker, 2016; Wan et al., 2022), following the thermal–optical

https://doi.org/10.5194/egusphere-2026-308
Preprint. Discussion started: 13 February 2026

transmittance method. Elemental composition of aerosol samples was analyzed by online X-ray fluorescence spectrometry (XRF) (Marguí et al., 2022), allowing quantification of a wide range of elements including light metals (K, Ca, etc.), metalloids (As, Se, etc.), and heavy metals (Zn, Pb, Cu, Hg, etc.).

2.2.3 Ice-nucleating particle (INP) concentration

N_{INP} were determined using the Peking University Ice Nucleation Array (PKU-INA), a cold-stage-based ice nucleation instrument (Chen et al., 2018, Chen et al., 2021). Each filter was fully immersed in 20 mL of double-distilled water (resistivity: 18.2 MΩ cm^{-1} at 25 °C), and were extracted using an ultrasonic shaker for 30 min. Ultrasonic extraction is an effective method for removing particles from filters (Ardon-Dryer and Levin, 2014; Chen et al., 2018; Reicher et al., 2019; Chen et al., 2021), although it may alter the bioactivity of proteins (De Leo et al., 2017). To minimize ultrasound-induced heating, the extraction was performed in a water bath with ice. The resulting suspension was dispensed into 90 droplets (1 µL each) on a hydrophobic glass slide. A metal spacer was placed on the slide to assist in droplet positioning and to suppress the Wegener–Bergeron–Findeisen process (Jung et al., 2012). A top glass was placed on the spacer to seal the droplets. The cold stage was first cooled from room temperature to 0 °C at 20 °C min^{-1}, and then at 1 °C min^{-1} until all droplets are frozen. The image of each droplet was recorded by a CCD camera every 6 seconds, corresponding to a temperature resolution of 0.1 °C. These images were later analyzed by customized software to identify the phase transition of each droplet by its brightness change upon freezing. High-purity dry nitrogen was used as sheath gas to prevent condensation and frost formation. The temperature uncertainty at the applied cooling rate was within ± 0.4 °C (Chen et al., 2018).

The cumulative number of ice-active sites per unit droplet volume above temperature T was calculated according to Vali et al. (2015):

$$K(T) = -\frac{\ln\left(1 - f_{\mathrm{ice}}(T)\right)}{V}\ (\mathrm{cm}^{-3}\ \text{of water}), \tag{1}$$

where $f_{ice}(T)$ is the fraction of droplets frozen at T, and V is the volume of each pipetted droplet (1 µL in this study). Combined with the total sampling volume, the $N_{INP}(T)$ per unit volume of sampled air is calculated as

$$N_{\mathrm{INP}}(T) = -\frac{\ln\left(1 - f_{\mathrm{ice}}(T)\right)}{V_{\mathrm{air}}}\ (\mathrm{L}^{-1}\ \text{air}), \tag{2}$$

where V_{air} is the total volume of sampled air per droplet converted to standard conditions (0 °C, 1013 hPa) during each sample collection period. To quantify and compare the ice-nucleating activity of aerosol particle with different size, the n_s (Vali et al., 2015), i.e., the cumulative ice-nucleation-active-site surface density (Connolly et al., 2009; Niedermeier et al., 2011; Hoose and Möhler, 2012), is calculated from the $N_{INP}(T)$ as

$$n_{\mathrm{s}}(T) = \frac{N_{\mathrm{INP}}(T)}{A}\ (\mathrm{m}^{-2}), \tag{3}$$

where A is the total surface area of the particles per unit volume of sampled air, derived from size distribution measurements of the particles. Note that aerodynamic diameter was used in the calculation of $n_s(T)$.

https://doi.org/10.5194/egusphere-2026-308
Preprint. Discussion started: 13 February 2026

The main source of uncertainty in the experimental results stems from the statistical representativeness of the droplets analyzed relative to the entire particle suspension. Due to the low ambient concentrations of INPs, the number of INPs present in the resulting particle suspension is typically small. As each droplet has a volume of only 1 μL, individual droplets may not adequately reflect the true particle distribution in the bulk extract. Moreover, the total number of droplets tested per sample (90 in this study) imposes a statistical limitation. To account for this, confidence intervals for the estimated INP concentration per droplet (and per unit sample volume) were calculated following the statistical approach described in previous studies (Barker, 2002; O'Sullivan et al., 2018), as shown in Eq. (4):

$$\mu(T) + \frac{\left(Z_{\alpha/2}\right)^2}{2n} \pm Z_{\alpha/2}\left[4\mu + \frac{\left(Z_{\alpha/2}\right)^2}{2n}\right]^{0.5} /(4n)^{0.5} \quad (4)$$

where $\mu(T)$ represents the number of INPs per droplet, n is the total number of droplets analyzed, and $Z_{\alpha/2}$ denotes the standard normal score corresponding to the desired confidence level (1.96 for a 95 % confidence interval).

For each aerosol sample, the parameters ($f_{ice}(T)$, $K(T)$, $N_{INP}(T)$, $n_s(T)$, and uncertainty) were calculated individually. The $f_{ice}(T)$ was derived from cold-stage measurements, V_{air} was obtained from recorded sampling volumes, and A was calculated based on concurrent SMPS data.

2.2.4 Air mass backward trajectory analysis

Backward trajectory analysis and visualization were performed using the MeteoInfoMap program (Wang, 2014), which is based on the HYSPLIT4 (Hybrid Single Particle Lagrangian Integrated Trajectory) model developed by the NOAA (National Oceanic and Atmospheric Administration, USA) Air Resources Laboratory. The analysis used GDAS (Global Data Assimilation System, 1°, global) meteorological data from NOAA (Stein et al., 2015). Trajectories were calculated with a duration of 72 h and an interval of 6 h between each trajectory, arriving at an altitude of 850 m above sea level (a.s.l.).

2.2.5 Positive matrix factorization (PMF)

The Positive Matrix Factorization (PMF) model was applied to analyze the sources of $PM_{2.5}$. PMF is a widely used receptor model for source apportionment. It can identify the composition and contribution of various sources. The model assumes that species emitted from the same source exhibit strong correlations, enabling the extraction of meaningful factors from measured concentration data (Karagulian et al., 2015; US EPA, 2015).

Given an $i \times j$ matrix $\mathbf{X}$ consisting of concentrations of j chemical species across i samples, PMF decomposes the matrix into two positive matrices—factor contributions ($\mathbf{G}$) and factor profiles ($\mathbf{F}$)—according to Equation (5):

$$\boldsymbol{X}_{ij} = \sum_{k=1}^{p} \boldsymbol{G}_{ik}\boldsymbol{F}_{kj} + \boldsymbol{E}_{ij} \quad (5)$$

https://doi.org/10.5194/egusphere-2026-308
Preprint. Discussion started: 13 February 2026

where p is the number of factors, i denotes the sample index, and j represents the species index. $\boldsymbol{X}_{ij}$ is the measured concentration of species j in sample i; $\boldsymbol{G}_{ik}$ represents the contribution of factor k to sample i; $\boldsymbol{F}_{jk}$ is the mass fraction of species j in factor k; and $\boldsymbol{E}_{ij}$ denotes the residuals. Both $\boldsymbol{G}_{ik}$ and $\boldsymbol{F}_{jk}$ are constrained to be non-negative.

To obtain the optimal solution, PMF minimizes an objective function Q (Eq. 6) using uncertainty estimates u_{ij} and non-negativity constraints on $\boldsymbol{G}$ and $\boldsymbol{F}$:

$$Q = \sum_{i=1}^{m}\sum_{j=1}^{n}\left(\frac{\boldsymbol{X}_{ij} - \sum_{k=1}^{p}\boldsymbol{G}_{ij}\boldsymbol{F}_{kj}}{u_{ij}}\right)^2 \quad (6)$$

The uncertainty u_{ij} is estimated following the EPA PMF 5.0 User Guide (US EPA, 2015) as:

$$u_{ij} = \begin{cases} \frac{5}{6} \times \mathrm{MDL} \ \ (c \le \mathrm{MDL}) \\ \sqrt{\left(ef \times \boldsymbol{X}_{ij}\right)^2 + (0.5 \times \mathrm{MDL})^2} \ \ (c > \mathrm{MDL}) \end{cases} \quad (7)$$

where c is the measured concentration of a given species, MDL is the method detection limit, and ef is the analytical uncertainty, typically between 0.05 and 0.2. In this study, $ef = 0.1$ was applied.

EPA PMF 5.0 software was employed for source apportionment of $PM_{2.5}$ in the study region. The specific datasets and their sources used for PMF analysis are described in Section 3.4. To determine the optimal number of factors, 4-7 factors were tested with 20 iterative runs each, and the solution with the most physically interpretable source profiles and lowest residuals was selected for final analysis (US EPA, 2015). Consequently, a five-factor solution was determined to be the optimal choice.

3 Results and discussion

3.1 Overview of INP temporal variability and aerosol characteristics

Figure 1 presents the temporal evolution of atmospheric INP concentrations and relevant aerosol parameters during the observation period in Taiyuan, including size-segregated particle number concentrations, carbonaceous components (OC and EC), as well as mass concentrations of $PM_{2.5}$ and PM_{10}, and water-soluble ions. Daily N_{INP} at different temperatures are shown in Fig. 1a (data for 15, 16, and 19 December are missing). At −15 °C, N_{INP} ranged from 10^{-2} to 10^{1} L^{-1} with a mean of 1.75 L^{-1}. Correspondingly, n_s values spanned 10^5 to 10^7 m^{-2}, with a mean of 3.89×10^6 m^{-2}.

Several distinct events can be identified throughout the campaign, as highlighted in Fig. 1. The first event (5-9 December, orange shading) was characterized by a sharp increase in coarse-mode (here defined as particles with aerodynamic diameter >1 μm, $N_{>1\,\mu m}$) particle concentrations (Figs. 1b, S1b, and S2). During this episode, the mean $N_{>1\mu m}$ increased to 5.94 cm^{-3}, which was approximately 2.7 times higher than the average concentration during the non-dust period (2.21 cm^{-3}). A peak daily concentration of 12.08 cm^{-3} was recorded on 6 December, accompanied by a steep rise in PM_{10} that reached nearly 800 μg m^{-3} (Figs. 1b and 1d).

https://doi.org/10.5194/egusphere-2026-308
Preprint. Discussion started: 13 February 2026

72-hour back trajectory analysis by HYSPLIT model confirmed that air masses during this period predominantly originated from the Taklamakan, Gurbantünggüt, or Badain Jaran Deserts in northwestern China, with trajectory paths highly overlapping the desert regions (Fig. S3). This pattern is consistent with desert dust transport events previously observed in northern China (Chen et al., 2021), confirming the influence of desert dust plume. Given the well-established high ice-nucleating activity of mineral dust, this episode is identified as a desert dust-intrusion event responsible for the pronounced enhancement in N_{INP}, especially at temperatures > −12.5 °C. Further discussion of its characteristics and implications is provided in Section 3.2.

Other episodes (13-14, 18, and 28-30 December, gray shading) were characterized by simultaneous increases in sulfate, nitrate, ammonium, and organic carbon, accompanied by elevated $PM_{2.5}$ and PM_{10} levels (Fig. 1c and Fig. 1d). This indicates the influence of air pollution driven by regional secondary aerosol accumulation under stagnant winter meteorology. Moderate N_{INP} increases were observed during the earlier two episodes (13–14 and 18 December), suggesting that secondary aerosol formation may indirectly modulate ice-nucleating activity through coating or mixing with pre-existing ice-active particles. The late-December event showed no corresponding N_{INP} enhancement despite high PM levels, indicating that aerosol mass concentration alone may not determine INP abundance. This contrast emphasizes that particle composition and surface properties, rather than overall pollution intensity, govern INP activity during secondary pollution periods (Chen et al., 2018; Wagh et al., 2021; Zhang et al., 2022).

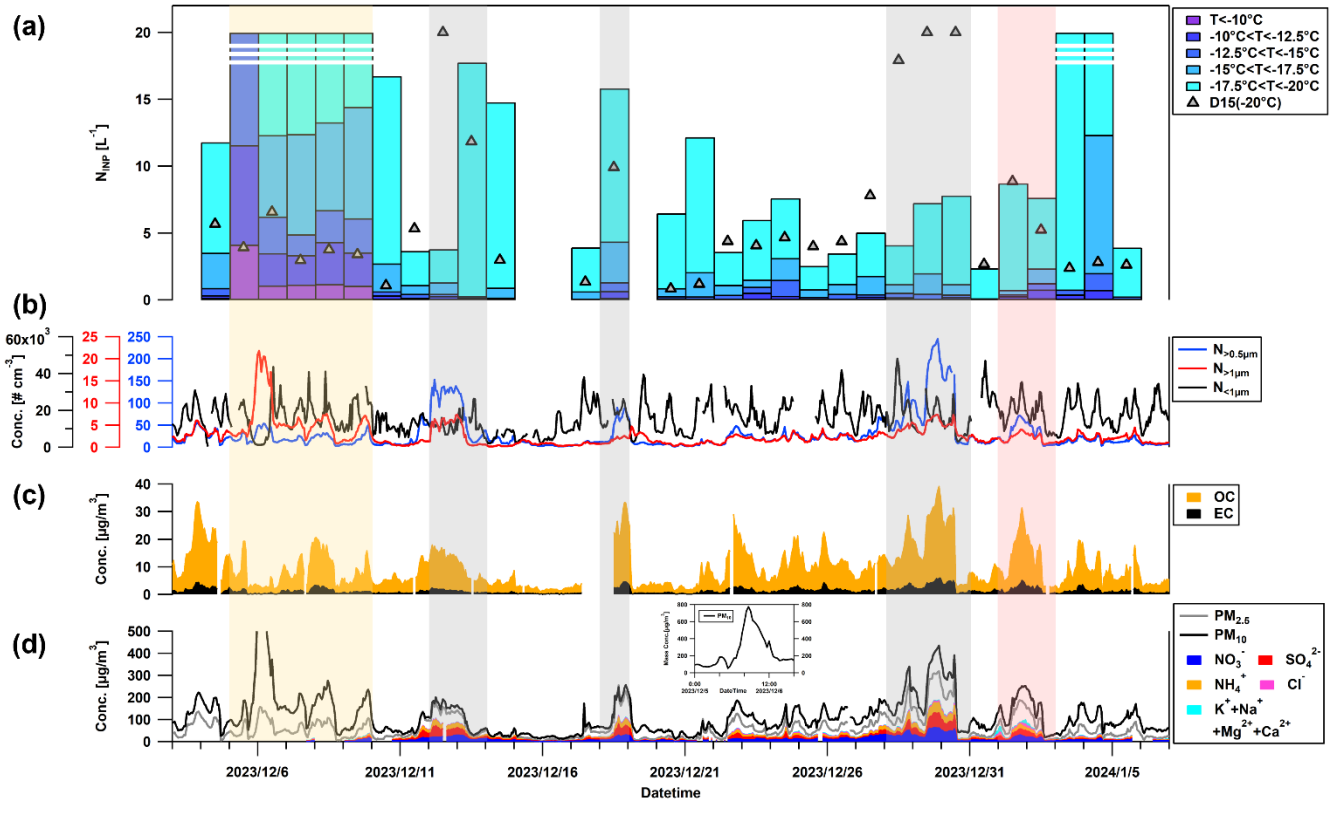

https://doi.org/10.5194/egusphere-2026-308
Preprint. Discussion started: 13 February 2026

Figure 1. Time series of (a) temperature-resolved N_{INP}, (b) size-resolved particle number concentrations, (c) mass concentrations of OC and EC, and (d) Mass concentrations of $PM_{2.5}$ and PM_{10} and major water-soluble ions (K^+, Na^+, Mg^{2+}, Ca^{2+}, Cl^-, NH_4^+, SO_4^{2-}, NO_3^-) determined by MARGA during the observation period. In panel (a), gray triangles (D15(–20°C)) represent values calculated using the N_{INP} parameterization scheme proposed by DeMott et al. (2015). Desert dust periods are shown in light orange, pollution periods in light gray, and fireworks events in light red.

Around 2 January 2024 (light-red shading), a short-lived pollution event occurred, accompanied by sharp increases in PM mass and concurrent peaks in K, OC, EC, Cu, and Sr (Figs. 1c and 1d), species indicative of firework emissions during New Year celebrations. Despite elevated particle concentrations and combustion-related aerosol components, N_{INP} remained low, suggesting that freshly emitted anthropogenic particles, including black carbon and other combustion products, are relatively inefficient as INPs, consistent with previous observations that even locally high concentrations of combustion aerosols contribute little to atmospheric ice-nucleating activity (Adams et al., 2020; Zhang et al., 2022).

3.2 Comparison with previous urban studies and parameterizations

Figure 2 compares the measured N_{INP} in this study with values reported previously. All samples in Taiyuan activated before −15 °C, with the most active samples initiating freezing near –5°C. The N_{INP} varied by more than two orders of magnitude among different samples, particularly in the −10 °C to −15 °C range, where values ranged from below 0.01 L^{-1} to above 10 L^{-1}. Such variability primarily reflects the influence of the desert dust intrusion identified earlier (highlighted in darker orange in Fig. 2), during which enhanced N_{INP} values were observed due to long-range transport of natural mineral particles.

Compared with other observations, the N_{INP} measured in non-desert-dust period (excluding the dust event of 5–9 December) in Taiyuan is roughly one order of magnitude higher than that measured at urban sites in Tokyo (Tobo et al., 2020) within the −10 °C to −25 °C range, while it is comparable to observations from Sisal, Mexico (Ladino et al., 2016), and New Delhi, India (Wagh et al., 2021) between −15°C to −20°C. In contrast, N_{INP} measured during Beijing summer time (Chen et al., 2024) is comparable to the lower bound of the Taiyuan data. Chen et al. (2024) found that anthropogenic dust particles, such as road dust influenced by traffic emissions, are important INP sources in the urban atmosphere. This implies that the INPs observed in Taiyuan may also be influenced by anthropogenic dust particles.

The linear N_{INP} parameterizations derived from field measurements in Beijing (Bi et al., 2018) and Huangshan (Su et al., 2014) also capture the overall magnitude of the present measurements. Although the N_{INP} levels in Taiyuan are relatively high compared with other urban observations, they are broadly comparable with those reported in other relevant studies. Additionally, the gray shaded area denotes the N_{INP} range derived from precipitation samples summarized by Petters and Wright (2015), which represents background INP activity in relatively clean environments. The Taiyuan N_{INP} obtained above −15 °C fall mostly within this area, indicating that during non-desert-dust periods, the warm-temperature N_{INP} in Taiyuan does not exceed the upper bound of global background levels. At colder temperatures, however, the measured N_{INP} values exceed this range substantially, suggesting additional contributions from ice-active components or enhanced influence of transported desert dust during certain periods. Taken together, these features indicate that the INP population in Taiyuan is governed by two distinct regimes: while episodic desert dust transport drives the most prominent peaks in concentration, the observed

https://doi.org/10.5194/egusphere-2026-308
Preprint. Discussion started: 13 February 2026

variability during non-dust periods is primarily shaped by local anthropogenic emissions, which maintain a fluctuating but relatively elevated background level.

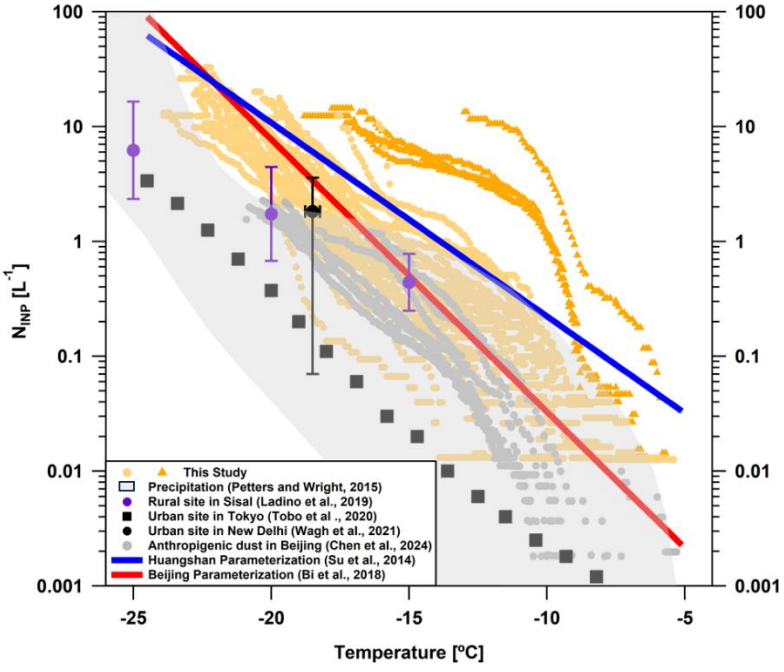

Figure 2. Comparison of N_{INP} obtained in this study with those reported in previous studies. Pale-yellow circles represent N_{INP} values from this study during non-desert-dust periods, while orange triangles denote data collected during dust intrusion events. Gray circles show anthropogenic-dust samples collected in Beijing (Chen et al., 2024). Solid red and blue lines correspond to parameterizations for Beijing and Huangshan (Bi et al., 2018; Su et al., 2014). Black squares and circles denote average N_{INP} values measured in Tokyo (Tobo et al., 2020) and New Delhi (Wagh et al., 2021), respectively; purple circles indicate data from Sisal, Mexico (Ladino et al., 2019). The light-gray shaded area shows N_{INP} ranges from precipitation samples (Petters and Wright, 2015).

3.3 Characterization of dust INPs

During the desert dust event (5–9 December; light-gray shading in Fig. 1a), both N_{INP} and n_s increased markedly. At −15 °C, N_{INP} reached 13.4 L^{-1} and n_s peaked at 3.49 × 10^7 m^{-2}, while their mean values rose from 1.75 L^{-1} to 7.47 L^{-1} and from 3.89 × 10^6 m^{-2} to 1.77 × 10^7 m^{-2}, respectively. These coherent increases in concentration and surface-active-site density indicate that the episode was characterized by both an increased abundance of INPs and substantially enhanced intrinsic ice-nucleating activity. Figure 1a also compares the measurements with the DeMott et al. (2015) parameterization (D15), which links INP concentrations to the number concentration of particles larger than 0.5 μm. While D15 captures the correct order of magnitude, it tends to underestimate the INP peak during the desert dust event (5–9 December) and overestimate INP concentrations during the pollution episode (28–30 December). This discrepancy suggests that coarse-particle abundance alone may not fully constrain INP variability in Taiyuan. Unlike typical urban environments where construction dust or road dust is a primary coarse-mode contributor (Chen et al., 2024), particles larger than 0.5 μm in Taiyuan are likely dominated by local surface emissions from the surrounding Loess Plateau and fugitive dust from intensive industrial activities (e.g., mining and

https://doi.org/10.5194/egusphere-2026-308
Preprint. Discussion started: 13 February 2026

285 production). The apparent overestimation by D15 during pollution episodes implies that these locally sourced coarse particles
286 may possess lower ice-nucleating efficiency compared to the highly active desert dusts assumed in the parameterization.
287 Therefore, while size-based parameterizations provide a useful approximation, incorporating source-specific or compositional
288 factors could further improve INP predictability in such complex industrial-urban environments.

289 Figure 3 compares n_s as a function of temperature for desert dust-affected samples (red) with non-desert-dust samples (blue).
290 Across the full temperature range, dust-affected samples exhibit systematically higher n_s values than non-dust samples.
291 Between −10 °C and −15 °C, desert dust-affected samples exhibited n_s values approximately one order of magnitude higher
292 than the most active non-desert-dust samples. In the colder range (−20 °C to −15 °C), most dust-affected samples fall within
293 about one order of magnitude of the desert-dust parameterizations proposed by Niemand et al. (2012) and Chen et al. (2021),
294 indicating ice-nucleating behavior consistent with long-range transported mineral dust. Considering that Taiyuan is located on
295 the western edge of the North China Plain while Beijing lies farther downwind, dust arriving in Beijing typically experiences
296 a longer transport history and stronger atmospheric aging. However, as shown in Fig. 3, the Beijing dust parameterization
297 closely overlaps with the n_s values of the dust samples in this study across the entire temperature range, without exhibiting
298 notable suppression of activity. This comparison suggests that, under the East Asian desert dust transport regime, typical
299 atmospheric aging does not significantly modify the surface ice-nucleating activity of mineral dust, and that mineralogical
300 composition and particle-size characteristics are likely more important determinants. Existing studies further indicate that
301 atmospheric oxidation processes can produce inconsistent effects on the heterogeneous freezing ability of mineral dust—
302 ranging from slight enhancement to modest inhibition—and their overall impact remains uncertain (Kanji et al., 2013).

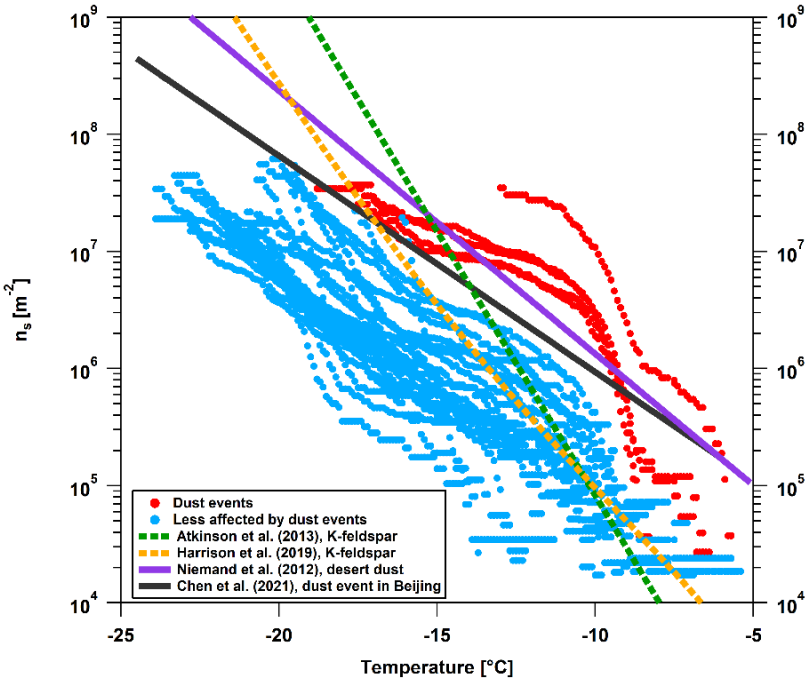

303

https://doi.org/10.5194/egusphere-2026-308
Preprint. Discussion started: 13 February 2026

Figure 3. Comparison of n_s obtained in this study with those reported in previous studies. Blue and red markers represent the n_s values of samples from this study that were less affected and affected by dust transport, respectively. The solid lines show n_s parameterizations for dust or individual mineral components reported in previous studies (Atkinson et al., 2013; Chen et al., 2021; Harrison et al., 2019; Niemand et al., 2012).

It is also noteworthy that at relatively warm temperatures (approximately $T > -12$ °C), n_s values of the ambient desert dust samples substantially exceed the parameterizations for pure K-feldspar (Atkinson et al., 2013; Harrison et al., 2019), suggesting that mineralogy alone cannot account for the elevated warm-temperature activity. Previous laboratory and field studies have shown that mineral dust particles can act synergistically with biological macromolecules or cellular fragments, leading to pronounced enhancement of heterogeneous freezing at warmer temperatures (Augustin-Bauditz et al., 2016; O'Sullivan et al., 2016; Yahya et al., 2019). The enhanced n_s observed at $T > -12$ °C in this study is therefore likely to reflect the combined influence of mineral dust and potentially co-transported biological INP components, rather than mineral dust alone.

3.4 Anthropogenic particle pollution affecting INP concentrations during non-dust periods

The Pearson correlation coefficients between N_{INP} at different temperatures and various pollutants were calculated for non-desert-dust periods. As shown in Table S1, only Ca, Co, Ni, and Au exhibited statistically significant correlations ($p < 0.05$; $n = 24$). The mean concentrations of Co, Ni, and Au were all below 10 ng m^{-3}, suggesting that their correlations are of limited physical relevance. By contrast, Ca averaged about 405 ng m^{-3} but was notably correlated only with N_{INP} at −10 °C. As a typical crustal element, Ca is closely linked to particles larger than 1 μm (Chen et al., 2024). Excluding the influence of long-range dust transport, this observation likely points to contributions from local surface emissions from the surrounding Loess Plateau and fugitive dust from industrial activities, rather than typical urban construction dust.

The weak correlations for all pollutants highlight that individual chemical species provide limited explanatory power for INP variability during non-desert-dust periods. This reflects the fact that INPs constitute only a minor and compositionally distinct subset of the total aerosol population, and thus bulk pollutant concentrations are not expected to correlate strongly with N_{INP}. To further determine the relevant emission sources, PMF analysis was applied to the full chemical composition dataset, resolving five major factors (industry, dust-related, secondary aerosols, coal combustion and traffic, and fireworks). Note that data before December 9 are not shown, as only non-desert-dust periods were considered in the analysis. The "Dust related" factor exhibits characteristic chemical signatures of mineral dust (e.g., high loadings of Ca and Mg^{2+}). However, the absence of long-range transport signals during these periods suggests it primarily originates from local anthropogenic sources—specifically, a mixture of road dust, fugitive dust from industrial and construction activities, and locally resuspended soil, rather than natural desert dust. Notably, unlike the long-range transported dust, this local anthropogenic dust factor showed no significant correlation with INP abundance (Table 1). The reconstructed daily $PM_{2.5}$ contributions (Fig. 4) show that secondary aerosols and coal/traffic emissions dominate the mass burden throughout the campaign, whereas fireworks emissions become prominent during the New Year period.

https://doi.org/10.5194/egusphere-2026-308
Preprint. Discussion started: 13 February 2026

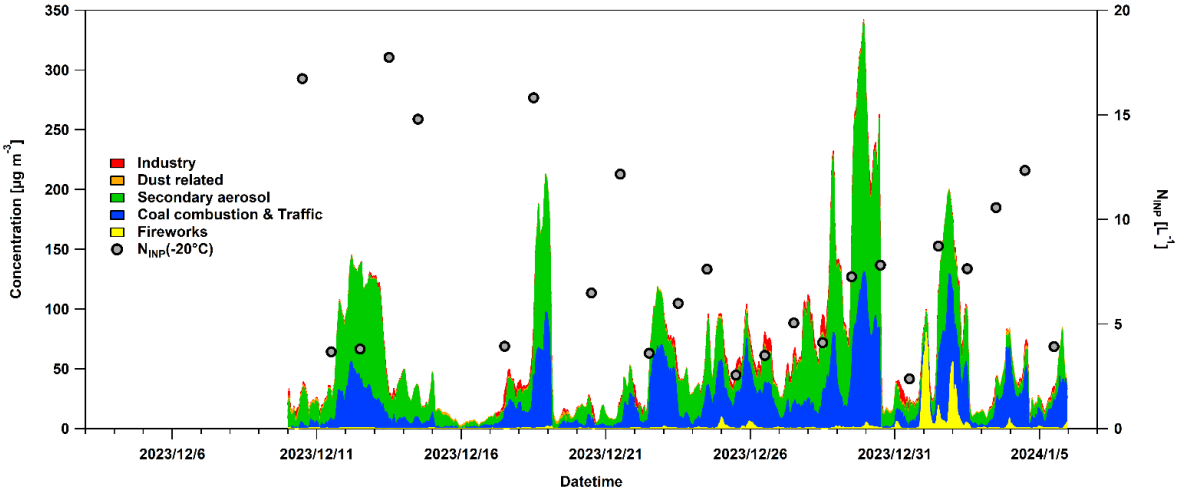

Figure 4. The daily $PM_{2.5}$ time series resolved using the PMF model is presented, with the corresponding N_{INP} at −20 °C also shown. The samples collected on December 13, 14, 21 and January 3, 4 were fully frozen before −20 °C, exceeding the quantifiable range of the assay.

To evaluate whether any of these major aerosol sources influence INP, Pearson correlations were calculated between N_{INP} at −20 °C and the time series of the PMF factors during non-dust periods (Table 1). All correlations were weak ($|r| < 0.3$) and statistically insignificant ($p > 0.05$), indicating no clear link between INP abundance and any of the dominant anthropogenic sources. Importantly, even during periods with strong increases in secondary inorganic and organic aerosols, such as 13–14 December, 18 December, and 28–30 December, N_{INP} did not rise proportionally (Fig. 4). This contrast underscores that urban pollution episodes are driven mainly by fine-mode, secondarily formed particles which, in contrast to mineral dust, do not substantially modify ambient INP levels (Kanji et al., 2017; Wagh et al., 2021; Zhang et al., 2022).

Table 1. Pearson correlation coefficients (r) and corresponding p-values between N_{INP}**(**−20 °C**)** and concentration contributions of PMF-resolved factors during non-dust periods.

Aerosol Source	Pearson r value	p value
Industry	-0.264	0.274
Dust related	0.210	0.389
Secondary aerosol	0.145	0.553
Coal & Traffic	0.034	0.892
Fireworks	0.108	0.659

These results collectively demonstrate that N_{INP} variability during non-dust periods is not controlled by major anthropogenic emission categories but instead emerges from the interplay of multiple factors, such as episodic inputs of local coarse-mode particles, variable physicochemical properties, and changes in atmospheric processing that modulate the availability of active surface sites. The absence of significant correlations with PMF-resolved sources also aligns with previous observations at urban sites worldwide, where the majority of anthropogenic aerosols contribute little to INP abundance, and INPs remain scarce and episodic relative to total aerosol loading.

https://doi.org/10.5194/egusphere-2026-308
Preprint. Discussion started: 13 February 2026

4 Conclusions

This study provides a detailed observational assessment of atmospheric INPs in Taiyuan, a heavily industrialized city in North China. By combining freezing assays, aerosol chemical composition, back-trajectory analysis, and PMF source apportionment, the work characterizes the concentration range, thermal activation behavior, and source influences of INPs in an urban environment where such information has been largely absent. The results establish a representative baseline for INP abundance in an industrial city and provide a framework for evaluating the contributions of local anthropogenic emissions versus naturally transported particles.

A key finding of this study is that the temporal variability of INP concentrations is dominated by episodic natural desert dust transport. During the 5–9 December desert dust event, N_{INP} and ns increased by up to an order of magnitude and freezing initiated at markedly warmer temperatures. Back trajectories confirmed that these highly active samples were associated with air masses originating from the major desert regions in northwestern China. Comparison with previously reported dust parameterizations indicates that the transported desert dust retained strong ice-nucleating activity despite longer atmospheric residence times, suggesting that typical aging processes do not substantially suppress the INP efficiency of East Asian mineral dust.

In contrast, during non-desert-dust periods, N_{INP} remained relatively low and showed weak correlations with common urban aerosol species. PMF analysis resolved five major $PM_{2.5}$ source factors: coal and traffic emissions, industrial processes, anthropogenic dust, secondary aerosols and fireworks, with secondary aerosols and coal/traffic contributions dominating the particle mass. Although secondary aerosols and coal/traffic emissions dominated $PM_{2.5}$ mass, none of these sources exhibited a significant influence on INP concentrations, demonstrating that the dominant contributors to $PM_{2.5}$ do not necessarily influence INP abundance. These results reinforce that INPs constitute a small and compositionally distinct subset of the aerosol population, and that no single anthropogenic source exerts primary control on urban INP variability.

The findings show that long-range desert dust transport is the decisive driver of INP enhancements in Taiyuan, whereas local anthropogenic emissions alone cannot account for observed INP behavior. The results also indicate that the complex and abundant anthropogenic emissions in urban environments provide a unique setting to examine the ice-nucleating activity of human-generated aerosols. These observations help clarify the relative contributions of natural and anthropogenic sources to INPs, and offer observational constraints for improving INP parameterizations in chemical transport and climate models.

Data availability

Data inquiries can be directed to the corresponding author (Zhijun Wu, zhijunwu@pku.edu.cn).

https://doi.org/10.5194/egusphere-2026-308
Preprint. Discussion started: 13 February 2026

Author contributions

JY, JingC and ZW designed experiments and methodology. JY, WF, JingC and ZF conducted the field observation. JY, ZW, WF, ZF, TZ, YQ, JunW and RM performed aerosol chemical and size distribution analyses; specifically, YQ was responsible for PMF (Positive Matrix Factorization) analysis, while JunW and RM assisted with offline sampling and chemical component analysis. JY, JieC and JingC calibrated the PKU-INA. TZ and WF provided meteorological data. MH, ZW and NT supervised the observation. JY, ZW, JieC and JingC prepared the article with input from all co-authors.

Competing interests

The authors declare that they have no conflict of interest.

Acknowledgements

We thank Ling Mu, Jiajie Li, Ying Wei, and Chenhui Li (Taiyuan University of Technology) for collecting the offline membrane samples.

Financial support

This work was supported by National Natural Science Foundation of China (NSFC, grant No. 42375093) and the cooperative research programs of Institute of Nature and Environmental Technology, Kanazawa University, Japan (25001, 25015).

References

Adams, M. P., Tarn, M. D., Sanchez-Marroquin, A., Porter, G. C. E., O'Sullivan, D., Harrison, A. D., Cui, Z., Vergara-Temprado, J., Carotenuto, F., Holden, M. A., Daily, M. I., Whale, T. F., Sikora, S. N. F., Burke, I. T., Shim, J.-U., McQuaid, J. B., and Murray, B. J.: A Major Combustion Aerosol Event Had a Negligible Impact on the Atmospheric Ice-Nucleating Particle Population, Journal of Geophysical Research: Atmospheres, 125, e2020JD032938, https://doi.org/10.1029/2020JD032938, 2020.

Ansmann, A., Tesche, M., Althausen, D., Müller, D., Seifert, P., Freudenthaler, V., Heese, B., Wiegner, M., Pisani, G., Knippertz, P., and Dubovik, O.: Influence of Saharan dust on cloud glaciation in southern Morocco during the Saharan Mineral Dust Experiment, Journal of Geophysical Research: Atmospheres, 113, https://doi.org/10.1029/2007JD008785, 2008.

Ardon-Dryer, K. and Levin, Z.: Ground-based measurements of immersion freezing in the eastern Mediterranean, Atmospheric Chemistry and Physics, 14, 5217–5231, https://doi.org/10.5194/acp-14-5217-2014, 2014.

Atkinson, J. D., Murray, B. J., Woodhouse, M. T., Whale, T. F., Baustian, K. J., Carslaw, K. S., Dobbie, S., O'Sullivan, D., and Malkin, T. L.: The importance of feldspar for ice nucleation by mineral dust in mixed-phase clouds, Nature, 498, 355–358, https://doi.org/10.1038/nature12278, 2013.

https://doi.org/10.5194/egusphere-2026-308
Preprint. Discussion started: 13 February 2026

Augustin-Bauditz, S., Wex, H., Kanter, S., Ebert, M., Niedermeier, D., Stolz, F., Prager, A., and Stratmann, F.: The immersion mode ice nucleation behavior of mineral dusts: A comparison of different pure and surface modified dusts, Geophysical Research Letters, 41, 7375–7382, https://doi.org/10.1002/2014GL061317, 2014.

Augustin-Bauditz, S., Wex, H., Denjean, C., Hartmann, S., Schneider, J., Schmidt, S., Ebert, M., and Stratmann, F.: Laboratory-generated mixtures of mineral dust particles with biological substances: characterization of the particle mixing state and immersion freezing behavior, Atmospheric Chemistry and Physics, 16, 5531–5543, https://doi.org/10.5194/acp-16-5531-2016, 2016.

Barker, L.: A Comparison of Nine Confidence Intervals for a Poisson Parameter When the Expected Number of Events is ≤ 5, The American Statistician, https://doi.org/10.1198/000313002317572736, 2002.

Bi, K., Ma, X., Chen, Y., Fu, S., and Xue, H.: The Observation of Ice-Nucleating Particles Active at Temperatures above–15°C and Its Implication on Ice Formation in Clouds, J Meteorol Res, 32, 734–743, https://doi.org/10.1007/s13351-018-7181-z, 2018.

Cabrera-Segoviano, D., Pereira, D. L., Rodriguez, C., Raga, G. B., Miranda, J., Alvarez-Ospina, H., and Ladino, L. A.: Inter-annual variability of ice nucleating particles in Mexico city, Atmospheric Environment, 273, 118964, https://doi.org/10.1016/j.atmosenv.2022.118964, 2022.

Chen, J., Wu, Z., Augustin-Bauditz, S., Grawe, S., Hartmann, M., Pei, X., Liu, Z., Ji, D., and Wex, H.: Ice-nucleating particle concentrations unaffected by urban air pollution in Beijing, China, Atmospheric Chemistry and Physics, 18, 3523–3539, https://doi.org/10.5194/acp-18-3523-2018, 2018.

Chen, J., Wu, Z., Chen, J., Reicher, N., Fang, X., Rudich, Y., and Hu, M.: Size-resolved atmospheric ice-nucleating particles during East Asian dust events, Atmospheric Chemistry and Physics, 21, 3491–3506, https://doi.org/10.5194/acp-21-3491-2021, 2021.

Chen, J., Wu, Z., Gong, X., Qiu, Y., Chen, S., Zeng, L., and Hu, M.: Anthropogenic Dust as a Significant Source of Ice-Nucleating Particles in the Urban Environment, Earth's Future, 12, e2023EF003738, https://doi.org/10.1029/2023EF003738, 2024.

Connolly, P. J., Möhler, O., Field, P. R., Saathoff, H., Burgess, R., Choularton, T., and Gallagher, M.: Studies of heterogeneous freezing by three different desert dust samples, Atmospheric Chemistry and Physics, 9, 2805–2824, https://doi.org/10.5194/acp-9-2805-2009, 2009.

De Leo, V., Catucci, L., Di Mauro, A. E., Agostiano, A., Giotta, L., Trotta, M., and Milano, F.: Effect of ultrasound on the function and structure of a membrane protein: The case study of photosynthetic Reaction Center from Rhodobacter sphaeroides, Ultrasonics Sonochemistry, 35, 103–111, https://doi.org/10.1016/j.ultsonch.2016.09.007, 2017.

DeMott, P. J., Prenni, A. J., Liu, X., Kreidenweis, S. M., Petters, M. D., Twohy, C. H., Richardson, M. S., Eidhammer, T., and Rogers, D. C.: Predicting global atmospheric ice nuclei distributions and their impacts on climate, Proceedings of the National Academy of Sciences, 107, 11217–11222, https://doi.org/10.1073/pnas.0910818107, 2010.

DeMott, P. J., Prenni, A. J., McMeeking, G. R., Sullivan, R. C., Petters, M. D., Tobo, Y., Niemand, M., Möhler, O., Snider, J. R., Wang, Z., and Kreidenweis, S. M.: Integrating laboratory and field data to quantify the immersion freezing ice nucleation activity of mineral dust particles, Atmospheric Chemistry and Physics, 15, 393–409, https://doi.org/10.5194/acp-15-393-2015, 2015.

https://doi.org/10.5194/egusphere-2026-308
Preprint. Discussion started: 13 February 2026

Engelstaedter, S., Tegen, I., and Washington, R.: North African dust emissions and transport, Earth-Science Reviews, 79, 73–100, https://doi.org/10.1016/j.earscirev.2006.06.004, 2006.

Harrison, A. D., Lever, K., Sanchez-Marroquin, A., Holden, M. A., Whale, T. F., Tarn, M. D., McQuaid, J. B., and Murray, B. J.: The ice-nucleating ability of quartz immersed in water and its atmospheric importance compared to K-feldspar, Atmospheric Chemistry and Physics, 19, 11343–11361, https://doi.org/10.5194/acp-19-11343-2019, 2019.

Hoose, C. and Möhler, O.: Heterogeneous ice nucleation on atmospheric aerosols: a review of results from laboratory experiments, Atmospheric Chemistry and Physics, 12, 9817–9854, https://doi.org/10.5194/acp-12-9817-2012, 2012.

Huang, Y., Adebiyi, A. A., Formenti, P., and Kok, J. F.: Linking the Different Diameter Types of Aspherical Desert Dust Indicates That Models Underestimate Coarse Dust Emission, Geophysical Research Letters, 48, e2020GL092054, https://doi.org/10.1029/2020GL092054, 2021.

Intergovernmental Panel on Climate Change (IPCC) (Ed.): Clouds and Aerosols, in: Climate Change 2013 – The Physical Science Basis: Working Group I Contribution to the Fifth Assessment Report of the Intergovernmental Panel on Climate Change, Cambridge University Press, Cambridge, 571–658, https://doi.org/10.1017/CBO9781107415324.016, 2014.

Jahn, L. G., Polen, M. J., Jahl, L. G., Brubaker, T. A., Somers, J., and Sullivan, R. C.: Biomass combustion produces ice-active minerals in biomass-burning aerosol and bottom ash, Proceedings of the National Academy of Sciences, 117, 21928–21937, https://doi.org/10.1073/pnas.1922128117, 2020.

Jung, S., Tiwari, M. K., and Poulikakos, D.: Frost halos from supercooled water droplets, Proceedings of the National Academy of Sciences, 109, 16073–16078, https://doi.org/10.1073/pnas.1206121109, 2012.

Kanji, Z. A., Welti, A., Chou, C., Stetzer, O., and Lohmann, U.: Laboratory studies of immersion and deposition mode ice nucleation of ozone aged mineral dust particles, Atmospheric Chemistry and Physics, 13, 9097–9118, https://doi.org/10.5194/acp-13-9097-2013, 2013.

Kanji, Z. A., Ladino, L. A., Wex, H., Boose, Y., Burkert-Kohn, M., Cziczo, D. J., and Krämer, M.: Overview of Ice Nucleating Particles, Meteorological Monographs, 58, 1.1-1.33, https://doi.org/10.1175/AMSMONOGRAPHS-D-16-0006.1, 2017.

Karagulian, F., Belis, C. A., Dora, C. F. C., Prüss-Ustün, A. M., Bonjour, S., Adair-Rohani, H., and Amann, M.: Contributions to cities' ambient particulate matter (PM): A systematic review of local source contributions at global level, Atmospheric Environment, 120, 475–483, https://doi.org/10.1016/j.atmosenv.2015.08.087, 2015.

Ladino, L. A., Yakobi-Hancock, J. D., Kilthau, W. P., Mason, R. H., Si, M., Li, J., Miller, L. A., Schiller, C. L., Huffman, J. A., Aller, J. Y., Knopf, D. A., Bertram, A. K., and Abbatt, J. P. D.: Addressing the ice nucleating abilities of marine aerosol: A combination of deposition mode laboratory and field measurements, Atmospheric Environment, 132, 1–10, https://doi.org/10.1016/j.atmosenv.2016.02.028, 2016.

Ladino, L. A., Raga, G. B., Alvarez-Ospina, H., Andino-Enríquez, M. A., Rosas, I., Martínez, L., Salinas, E., Miranda, J., Ramírez-Díaz, Z., Figueroa, B., Chou, C., Bertram, A. K., Quintana, E. T., Maldonado, L. A., García-Reynoso, A., Si, M., and Irish, V. E.: Ice-nucleating particles in a coastal tropical site, Atmospheric Chemistry and Physics, 19, 6147–6165, https://doi.org/10.5194/acp-19-6147-2019, 2019.

Li, F., Yan, J., Wei, Y., Zeng, J., Wang, X., Chen, X., Zhang, C., Li, W., Chen, M., and Lü, G.: PM2.5-bound heavy metals from the major cities in China: Spatiotemporal distribution, fuzzy exposure assessment and health risk management, Journal of Cleaner Production, 286, 124967, https://doi.org/10.1016/j.jclepro.2020.124967, 2021.

https://doi.org/10.5194/egusphere-2026-308
Preprint. Discussion started: 13 February 2026

Lohmann, U. and Feichter, J.: Global indirect aerosol effects: a review, Atmospheric Chemistry and Physics, 5, 715–737, https://doi.org/10.5194/acp-5-715-2005, 2005.

Lohmann, U., Lüönd, F., and Mahrt, F.: An Introduction to Clouds: From the Microscale to Climate, Cambridge University Press, Cambridge, https://doi.org/10.1017/CBO9781139087513, 2016.

Marguí, E., Queralt, I., and de Almeida, E.: X-ray fluorescence spectrometry for environmental analysis: Basic principles, instrumentation, applications and recent trends, Chemosphere, 303, 135006, https://doi.org/10.1016/j.chemosphere.2022.135006, 2022.

McCluskey, C. S., DeMott, P. J., Prenni, A. J., Levin, E. J. T., McMeeking, G. R., Sullivan, A. P., Hill, T. C. J., Nakao, S., Carrico, C. M., and Kreidenweis, S. M.: Characteristics of atmospheric ice nucleating particles associated with biomass burning in the US: Prescribed burns and wildfires, Journal of Geophysical Research: Atmospheres, 119, 10458–10470, https://doi.org/10.1002/2014JD021980, 2014.

Murray, B. J., O'Sullivan, D., Atkinson, J. D., and Webb, M. E.: Ice nucleation by particles immersed in supercooled cloud droplets, Chem. Soc. Rev., 41, 6519–6554, https://doi.org/10.1039/C2CS35200A, 2012.

Niedermeier, D., Hartmann, S., Clauss, T., Wex, H., Kiselev, A., Sullivan, R. C., DeMott, P. J., Petters, M. D., Reitz, P., Schneider, J., Mikhailov, E., Sierau, B., Stetzer, O., Reimann, B., Bundke, U., Shaw, R. A., Buchholz, A., Mentel, T. F., and Stratmann, F.: Experimental study of the role of physicochemical surface processing on the IN ability of mineral dust particles, Atmospheric Chemistry and Physics, 11, 11131–11144, https://doi.org/10.5194/acp-11-11131-2011, 2011.

Niemand, M., Möhler, O., Vogel, B., Vogel, H., Hoose, C., Connolly, P., Klein, H., Bingemer, H., DeMott, P., Skrotzki, J., and Leisner, T.: A Particle-Surface-Area-Based Parameterization of Immersion Freezing on Desert Dust Particles, https://doi.org/10.1175/JAS-D-11-0249.1, 2012.

O'Sullivan, D., Murray, B. J., Ross, J. F., and Webb, M. E.: The adsorption of fungal ice-nucleating proteins on mineral dusts: a terrestrial reservoir of atmospheric ice-nucleating particles, Atmospheric Chemistry and Physics, 16, 7879–7887, https://doi.org/10.5194/acp-16-7879-2016, 2016.

O'Sullivan, D., Adams, M. P., Tarn, M. D., Harrison, A. D., Vergara-Temprado, J., Porter, G. C. E., Holden, M. A., Sanchez-Marroquin, A., Carotenuto, F., Whale, T. F., McQuaid, J. B., Walshaw, R., Hedges, D. H. P., Burke, I. T., Cui, Z., and Murray, B. J.: Contributions of biogenic material to the atmospheric ice-nucleating particle population in North Western Europe, Sci Rep, 8, 13821, https://doi.org/10.1038/s41598-018-31981-7, 2018.

Peters, T. M., OTT, D., and O'SHAUGHNESSY, P. T.: Comparison of the Grimm 1.108 and 1.109 Portable Aerosol Spectrometer to the TSI 3321 Aerodynamic Particle Sizer for Dry Particles, Ann Occup Hyg, 50, 843–850, https://doi.org/10.1093/annhyg/mel067, 2006.

Petters, M. D. and Wright, T. P.: Revisiting ice nucleation from precipitation samples, Geophysical Research Letters, 42, 8758–8766, https://doi.org/10.1002/2015GL065733, 2015.

Polen, M., Lawlis, E., and Sullivan, R. C.: The unstable ice nucleation properties of Snomax® bacterial particles, Journal of Geophysical Research: Atmospheres, 121, 11,666-11,678, https://doi.org/10.1002/2016JD025251, 2016.

Price, H. C., Baustian, K. J., McQuaid, J. B., Blyth, A., Bower, K. N., Choularton, T., Cotton, R. J., Cui, Z., Field, P. R., Gallagher, M., Hawker, R., Merrington, A., Miltenberger, A., Neely III, R. R., Parker, S. T., Rosenberg, P. D., Taylor, J. W., Trembath, J., Vergara-Temprado, J., Whale, T. F., Wilson, T. W., Young, G., and Murray, B. J.: Atmospheric Ice-Nucleating

https://doi.org/10.5194/egusphere-2026-308
Preprint. Discussion started: 13 February 2026

Particles in the Dusty Tropical Atlantic, Journal of Geophysical Research: Atmospheres, 123, 2175–2193, https://doi.org/10.1002/2017JD027560, 2018.

Pummer, B. G., Budke, C., Augustin-Bauditz, S., Niedermeier, D., Felgitsch, L., Kampf, C. J., Huber, R. G., Liedl, K. R., Loerting, T., Moschen, T., Schauperl, M., Tollinger, M., Morris, C. E., Wex, H., Grothe, H., Pöschl, U., Koop, T., and Fröhlich-Nowoisky, J.: Ice nucleation by water-soluble macromolecules, Atmospheric Chemistry and Physics, 15, 4077–4091, https://doi.org/10.5194/acp-15-4077-2015, 2015.

Reicher, N., Budke, C., Eickhoff, L., Raveh-Rubin, S., Kaplan-Ashiri, I., Koop, T., and Rudich, Y.: Size-dependent ice nucleation by airborne particles during dust events in the eastern Mediterranean, Atmospheric Chemistry and Physics, 19, 11143–11158, https://doi.org/10.5194/acp-19-11143-2019, 2019.

Rumsey, I. C. and Walker, J. T.: Application of an online ion-chromatography-based instrument for gradient flux measurements of speciated nitrogen and sulfur, Atmospheric Measurement Techniques, 9, 2581–2592, https://doi.org/10.5194/amt-9-2581-2016, 2016.

Rumsey, I. C., Cowen, K. A., Walker, J. T., Kelly, T. J., Hanft, E. A., Mishoe, K., Rogers, C., Proost, R., Beachley, G. M., Lear, G., Frelink, T., and Otjes, R. P.: An assessment of the performance of the Monitor for AeRosols and GAses in ambient air (MARGA): a semi-continuous method for soluble compounds, Atmospheric Chemistry and Physics, 14, 5639–5658, https://doi.org/10.5194/acp-14-5639-2014, 2014.

Stein, A. F., Draxler, R. R., Rolph, G. D., Stunder, B. J. B., Cohen, M. D., and Ngan, F.: NOAA's HYSPLIT Atmospheric Transport and Dispersion Modeling System, https://doi.org/10.1175/BAMS-D-14-00110.1, 2015.

Su, H., Yin, Y., Lu, C., Jiang, H., and Yang, L.: Development of new diffusion cloud chamber type and its observation study of ice nuclei in the Huangshan area, Chinese Journal of Atmospheric Sciences (in Chinese), 38, 386–398, https://doi.org/10.3878/j.issn.1006-9895.2013.12211, 2014.

Tobo, Y., Uetake, J., Matsui, H., Moteki, N., Uji, Y., Iwamoto, Y., Miura, K., and Misumi, R.: Seasonal Trends of Atmospheric Ice Nucleating Particles Over Tokyo, Journal of Geophysical Research: Atmospheres, 125, e2020JD033658, https://doi.org/10.1029/2020JD033658, 2020.

Toll, V., Rahu, J., Keernik, H., Trofimov, H., Voormansik, T., Manshausen, P., Hung, E., Michelson, D., Christensen, M. W., Post, P., Junninen, H., Murray, B. J., Lohmann, U., Watson-Parris, D., Stier, P., Donaldson, N., Storelvmo, T., Kulmala, M., and Bellouin, N.: Glaciation of liquid clouds, snowfall, and reduced cloud cover at industrial aerosol hot spots, Science, 386, 756–762, https://doi.org/10.1126/science.adl0303, 2024.

EPA Positive Matrix Factorization 5.0 Fundamentals and User Guide: https://www.epa.gov/air-research/epa-positive-matrix-factorization-50-fundamentals-and-user-guide, last access: 10 October 2025.

Vali, G., DeMott, P. J., Möhler, O., and Whale, T. F.: Technical Note: A proposal for ice nucleation terminology, Atmospheric Chemistry and Physics, 15, 10263–10270, https://doi.org/10.5194/acp-15-10263-2015, 2015.

Wagh, S., Singh, P., Ghude, S. D., Safai, P., Prabhakaran, T., and Kumar, P. P.: Study of ice nucleating particles in fog-haze weather at New Delhi, India: A case of polluted environment, Atmospheric Research, 259, 105693, https://doi.org/10.1016/j.atmosres.2021.105693, 2021.

Wan, Z., Song, K., Zhu, W., Yu, Y., Wang, H., Shen, R., Tan, R., Lv, D., Gong, Y., Yu, X., Chen, S., Zeng, L., Lou, S., Yu, Y., and Guo, S.: A Closure Study of Secondary Organic Aerosol Estimation at an Urban Site of Yangtze River Delta, China, Atmosphere, 13, 1679, https://doi.org/10.3390/atmos13101679, 2022.

https://doi.org/10.5194/egusphere-2026-308
Preprint. Discussion started: 13 February 2026

560 Westbrook, C. D. and Illingworth, A. J.: The formation of ice in a long-lived supercooled layer cloud, Quarterly Journal of the
561 Royal Meteorological Society, 139, 2209–2221, https://doi.org/10.1002/qj.2096, 2013.

562 Wiedensohler, A.: An approximation of the bipolar charge distribution for particles in the submicron size range, Journal of
563 Aerosol Science, 19, 387–389, https://doi.org/10.1016/0021-8502(88)90278-9, 1988.

564 Yahya, R. Z., Arrieta, J. M., Cusack, M., and Duarte, C. M.: Airborne Prokaryote and Virus Abundance Over the Red Sea,
565 Front. Microbiol., 10, https://doi.org/10.3389/fmicb.2019.01112, 2019.

566 Zhang, C., Wu, Z., Chen, J., Chen, J., Tang, L., Zhu, W., Pei, X., Chen, S., Tian, P., Guo, S., Zeng, L., Hu, M., and Kanji, Z.
567 A.: Ice-nucleating particles from multiple aerosol sources in the urban environment of Beijing under mixed-phase cloud
568 conditions, Atmospheric Chemistry and Physics, 22, 7539–7556, https://doi.org/10.5194/acp-22-7539-2022, 2022.

569 Zolles, T., Burkart, J., Häusler, T., Pummer, B., Hitzenberger, R., and Grothe, H.: Identification of Ice Nucleation Active Sites
570 on Feldspar Dust Particles, J. Phys. Chem. A, 119, 2692–2700, https://doi.org/10.1021/jp509839x, 2015.

571